Inorg. Chem. **2002**, *41*, 6397–6403

Structures of the BrF_4^+ and IF_4^+ Cations

Ashwani Vij,[†] Fook S. Tham,[§] Vandana Vij,[†] William W. Wilson,[†] and Karl O. Christe*[,†,‡]

Air Force Research Laboratory, Edwards Air Force Base, Edwards, California 93524, University of Southern California Loker Hydrocarbon Research Institute, University Park, Los Angeles, California 90089, and Department of Chemistry, University of California, Riverside, California 92521

Received July 24, 2002

The large discrepancies between the calculated and observed structures for BrF_4^+ and IF_4^+ (Christe, K. O.; Zhang, X.; Sheehy, J. A.; Bau, R. *J. Am. Chem. Soc.* **2001**, *123,* 6338) prompted a redetermination of the crystal structures of $BrF_4^+Sb_2F_{11}^-$ (monoclinic, $P2_1/c$, $a = 5.2289(6)$ Å, $b = 14.510(2)$ Å, $c = 14.194(2)$ Å, $\beta = 90.280(1)°$, $Z = 4$) and $IF_4^+SbF_6^-$ (orthorhombic, *Ibca*, $a = 8.2702(9)$ Å, $b = 8.3115(9)$ Å, $c = 20.607(2)$ Å, $Z = 8$). It is shown that for BrF_4^+, the large differences were mainly due to large errors in the original experimental data. For $IF_4^+SbF_6^-$, the geometry previously reported for IF_4^+ was reasonably close to that found in this study despite a very large *R*-factor of 0.15 and a refinement in an incorrect space group. The general agreement between the calculated and the redetermined geometries of BrF_4^+ and IF_4^+ is excellent, except for the preferential compression of one bond angle in each ion due to the influence of interionic fluorine bridges. In BrF_4^+, the fluorine bridges are equatorial and compress this angle. In IF_4^+, the nature of the fluorine bridges depends on the counterion, and either the axial (in $IF_4^+SbF_6^-$) or the equatorial (in $IF_4^+Sb_2F_{11}^-$) bond angle is preferentially compressed. Therefore, the geometries of the free ions are best described by the theoretical calculations.

Introduction

The halogen central atoms in binary halogen fluoride molecules and ions exhibit oxidation states ranging from (+I) to (+VII) and coordination numbers ranging from 1 to 8. These wide ranges render them ideal candidates for exploring molecular structure and bonding.[1−3] In a recent paper, the crystal structure of $ClF_4^+SbF_6^-$ has been reported, and the general trends within the isoelectronic series ClF_4^+, BrF_4^+, IF_4^+, and SF_4, SeF_4, TeF_4, have been evaluated.[4] Whereas the theoretical calculations agreed well with the experimental structures of the neutral molecules and resulted in smooth trends, the crystal structures previously reported for ClF_4^+,[4] BrF_4^+,[5] and IF_4^+ [6,7] strongly deviated from the theoretical predictions and resulted in erratic trends[4] (see Figure 1). Because the crystal structures for BrF_4^+ and IF_4^+ were of low accuracy, it was important to redetermine these structures and to resolve the apparent discrepancies between theory and experiment.

Experimental Section

Materials and Apparatus. The sample of $BrF_4^+Sb_2F_{11}^-$ was prepared as previously described.[8] Single crystals were obtained by slow sublimation at room temperature over a time period of 30 years. Single crystals of $IF_4^+SbF_6^-$ were obtained in the following manner. In a glovebox, a 2-fold excess of SbF_5 (19.27 mmol) was loaded into a prepassivated Teflon ampule, fitted with a Hoke stainless steel valve. The ampule was connected to a stainless steel vacuum line[9] and evacuated at −196 °C. Anhydrous HF (3 mL) was condensed onto the SbF_5, followed by freshly distilled IF_5 (9.50 mmol). The reaction mixture was allowed to warm to room temperature for 1 h. All volatile material was pumped off at room temperature for 12 h, leaving behind a white crystalline solid

* To whom correspondence should be addressed. E-mail: karl.christe@edwards.af.mil.
[†] Air Force Research Laboratory.
[§] University of California, Riverside.
[‡] University of Southern California.

(1) Christe, K. O.; Curtis, E. C.; Dixon, D. A. *J. Am. Chem. Soc.* **1993**, *115*, 1520.
(2) Christe, K. O. *Plenary Main Sect. Lect. Int. Congr. Pure. Appl. Chem., 24th, 1973* **1974**, *4*, 115.
(3) Christe, K. O.; Wilson, W. W.; Drake, G. W.; Dixon, D. A.; Boatz, J. A.; Gnann, R. *J. Am. Chem. Soc.* **1998**, *120*, 1520.
(4) Christe, K. O.; Zhang, X.; Sheehy, J. A.; Bau, R. *J. Am. Chem. Soc.* **2001**, *123*, 6338.
(5) Lind, M. D.; Christe, K. O. *Inorg. Chem.* **1972**, *11*, 608.
(6) Baird, H. W.; Giles, H. F. *Acta Crystallogr.* **1969**, *A25*, S115.
(7) Edwards, A. J.; Taylor, P. *J. Chem. Soc., Dalton Trans.* **1975**, 2174.
(8) Christe, K. O.; Sawodny, W. *Inorg. Chem.* **1973**, *12*, 2879.
(9) Christe, K. O.; Wilson, W. W.; Schack, C. J.; Wilson, R. D. *Inorg. Synth.* **1986**, *24*, 39.

10.1021/ic025900q CCC: $22.00
Published on Web 10/30/2002

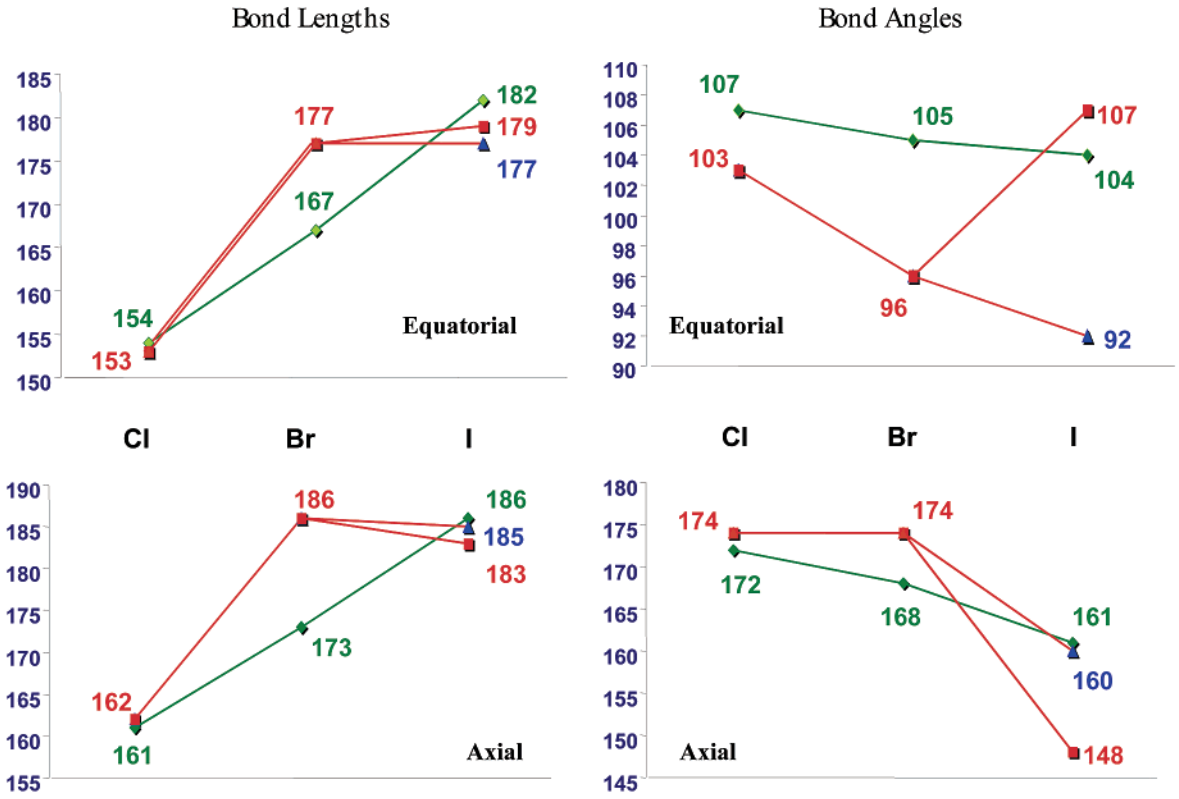

Figure 1. Comparison of calculated (green) and previously reported experimental (red and blue) geometries (distances in Å × 10^2, angles in deg) for ClF_4^+, BrF_4^+, and IF_4^+. For IF_4^+, the red values are those reported for $IF_4^+Sb_2F_{11}^-$,[7] while the blue ones are those for $IF_4^+SbF_6^-$.[6]

Table 1. Crystal Data for $BrF_4^+Sb_2F_{11}^-$ and $IF_4^+SbF_6^-$

	$BrF_4^+Sb_2F_{11}^-$	$IF_4^+SbF_6^-$
chemical formula	$BrF_{15}Sb_2$	$F_{10}ISb$
fw	608.41	438.65
T, K	243(2)	233(2)
space group	$P2_1/c$	*Ibca*
a, Å	5.2289(6)	8.2702(9)
b, Å	14.510(2)	8.3115(9)
c, Å	14.194(2)	20.607(2)
β, deg	90.280(2)	90
V, Å^3	1076.9 (2)	1416.5(3)
Z	4	8
μ, mm^{-1}	8.920	8.396
ρ_{calcd}, g cm^{-3}	3.753	4.114
R1,[a] wR2[b] [$I > 2\sigma(I)$]	0.0275, 0.0702	0.0241, 0.0654
R1,[a] wR2[b] (all data)	0.0344, 0.0735	0.0266, 0.0679

[a] $R1 = (\sum(F_o - F_c)/F_o)$. [b] $wR2 = [\sum(w(F_o - F_c)^2)w/F_o^2)]^{1/2}$.

identified as $IF_4^+SbF_6^-$ by material balance (9.50 mmol) and its infrared and Raman spectra.[8]

Crystal Structures of $BrF_4^+Sb_2F_{11}^-$ and $IF_4^+SbF_6^-$. Diffraction quality, colorless crystals of $BrF_4^+Sb_2F_{11}^-$ (**1**) or $IF_4^+SbF_6^-$ (**2**) were immersed into a perfluoro-polyether (PFPE) filled cavity of a culture dish. A crystal was then sucked by capillary force into a 0.3 mm Lindeman capillary tube along with some PFPE oil. The capillary was sealed at both ends and mounted on a goniometer head using a copper pin. The structures of the salts were determined with a Bruker CCD SMART 1000 diffractometer that was controlled by the SMART software.[10] Unit cell parameters were determined at 243 K ($BrF_4^+Sb_2F_{11}^-$) or 233 K ($IF_4^+SbF_6^-$) from three runs of frame data with a scan speed of 30 sec/frame and 30 frames per data run. A complete hemisphere of data was collected at the described temperatures using 1271 frames at 30 s/frame, including 50 frames that were collected at the beginning and end of each data collection to monitor crystal decay. Data were integrated using the SAINT[11] software, and the raw data were corrected for absorption using the SADABS[12] program. The structures were solved with the SHELXS-97 program[13] employing the Patterson method and refined anisotropically with the SHELXL-97[14] software incorporated into the SHELXTL 5.1 program[15] (Table 1).

For $BrF_4^+Sb_2F_{11}^-$, the intensity statistics, that is, the $E^2 - 1$ values, indicated a centrosymmetric space group. Furthermore, the absence of 0k0 (k = odd) and h0l reflections (l = odd) showed the presence of a 2_1 screw axis and a c-glide plane parallel and perpendicular to the b-axis, respectively. The space group was thus unambiguously assigned as $P2_1/c$.

The determination of the space group for $IF_4^+SbF_6^-$ was not trivial. Initial frame data indicated a body-centered orthorhombic cell (space group *Ibca*) with the following axes, a = 8.270 Å, b = 8.3115 Å, c = 20.607 Å. Because the a and b values are quite similar, the possibility of a tetragonal unit cell was also examined but rejected on the basis of the R_{sym} value being twice as large. Furthermore, solution of the structure using the tetragonal option results in a disordered structure flawed by poor geometry, thermal parameters and associated errors, a higher R-value of 0.0675, a poor

(10) *SMART Software for the CCD Detector System*; Bruker AXS: Madison, WI, 1999.
(11) *SAINT Software for the CCD Detector System*; Bruker AXS: Madison, WI, 1999.
(12) *SADABS, Program for absorption correction for area detectors*, version 2.01; Bruker AXS: Madison, WI, 2000.
(13) Sheldrick, G. M. *SHELXS-97, Program for the Solution of Crystal Structure*; University of Göttingen: Göttingen, Germany, 1997.
(14) Sheldrick, G. M. *SHELXL-97, Program for the Refinement of Crystal Structure*; University of Göttingen: Göttingen, Germany, 1997
(15) *SHELXTL 5.10 for Windows NT, Program Library for Structure Solution and Molecular Graphics*; Bruker AXS: Madison, WI, 1997.

Table 2. Comparison of the Experimental and Calculated Geometries[a] for the XF_4^+ Cations (X = Cl, Br and I)

	$R(X-F_{ax})$	$R(X-F_{eq})$	$F_{ax}-X-F_{ax}$	$F_{eq}-X-F_{eq}$
$ClF_4^+SbF_6^-$ (expt, ref 4)	1.618(2)	1.530(2)	173.9(1)	103.1(1)
ClF_4^+ (gas)[b] (MP2)	1.612	1.543	172.3	107.1
B3LYP	1.635	1.577	172.2	107.8
CCSD(T)	1.615	1.557	171.4	107.7
$BrF_4^+Sb_2F_{11}^-$ (expt, ref 5)	1.86(12)	1.77(12)	173.5(61)	95.5(50)
(expt this work)	1.728(3), 1.729(3)	1.664(3), 1.667(2)	168.9(2)	97.5(2)
BrF_4^+ (gas)[b] (MP2)	1.728	1.672	168.2	104.9
B3LYP	1.749	1.700	168.8	104.9
CCSD(T)	1.732	1.682	1.672	105.4
$IF_4^+SbF_6^-$ (expt, ref 6)				
(expt, this work)	1.849(2)	1.798(2)	149.2(1)	103.1(1)
$IF_4^+Sb_2F_{11}^-$ (expt, ref 7)	1.87(4), 1.82(3)	1.76(3), 1.78(3)	160.3(1.2)	92.4(1.2)
IF_4^+ (gas)[b] (MP2)	1.861	1.818	161.2	103.8
B3LYP	1.875	1.838	158.3	106.8
CCSD(T)	1.863	1.823	160.3	104.2

[a] Bond distances in angstroms, angles in degrees. [b] Data from ref 4. The following basis sets were used for all calculations: Br, DFT-DZVP + f(0.552); I, DFT-DZVP + f(0.486); F, −311 + G(2d).

data-to-parameter ratio of 8.514, and a high residual electron density. On the other hand, choice of the body-centered orthorhombic cell results in an ordered structure that could be solved in the space group *Ibca* with a lower *R*-value (0.0241), higher data-to-parameter ratio, and good thermal and geometrical parameters. On the basis of these considerations and the observed systematic absences, *Icba* is the correct space group. Although the possibility of a C-centered super lattice cannot be ruled out, it was not further pursued because of satisfactory refinement in *Icba*.

The previously reported[6] tetragonal cell (space group *P*4/*mmm*) with $a = 5.863$ Å and $c = 10.303$ Å can be obtained by transformation of our orthorhombic cell by using a −0.5, −0.5, 0.0, 0.5, −0.5, 0.0, 0.0, 0.0, 0.5 matrix. This, however, skews the γ angle to 89.71° and can account for some of the problems encountered with the previous study.

Results and Discussion

Calculated Structures of the Free BrF_4^+ and IF_4^+ Cations. Ideally, the XF_4^+ cations possess pseudo-trigonal bipyramidal geometries of C_{2v} symmetry with the third equatorial position being occupied by a sterically active, free valence electron pair.

Because the free electron pair domain is more repulsive than those of the fluorine ligands, the angles of both the axial and the equatorial fluorine bond pairs are smaller than the ideal 180° and 120°, respectively. In Table 2, the previously observed[5,7] geometries are compared to the unscaled values calculated[4] for free BrF_4^+ and IF_4^+ at different levels of theory. As can be seen from Table 2 and Figure 1, the agreement between the previously reported experimental and the calculated values is very poor, even if empirical corrections of about 0.01−0.04 Å for the overestimates that are typical for each method[4] are applied to the bond lengths.

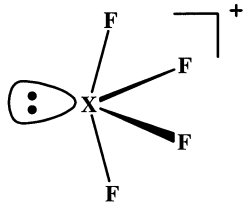

Crystal Structure of $BrF_4^+Sb_2F_{11}^-$. This compound crystallizes in the monoclinic space group $P2_1/c$. The earlier structural refinement[5] for this compound had used a nonstandard setting, $P2_1/a$, and the fluorine atoms had been refined isotropically, resulting in a high *R*-factor of 0.14 and very large uncertainties of up to 0.13 Å in the bond lengths. Therefore, the structure of $BrF_4^+Sb_2F_{11}^-$ was redetermined (Figure 2), and the atomic coordinates and isotropic displacement parameters are listed in Table 3. The most important

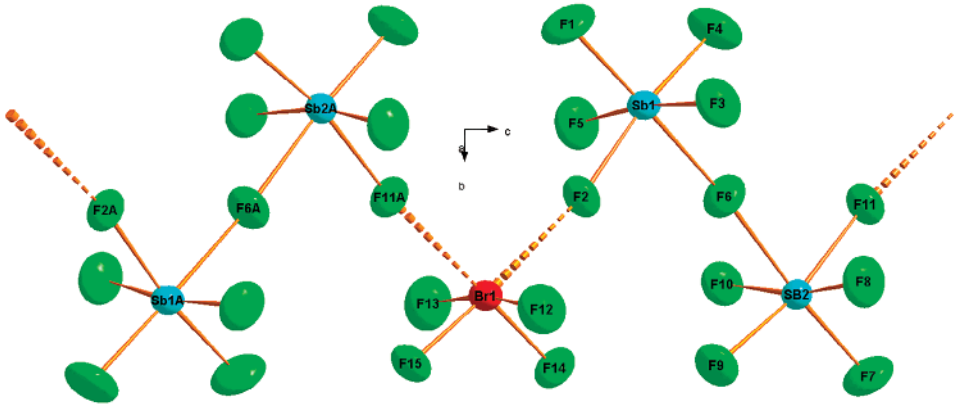

Figure 2. Crystal structure of $BrF_4^+Sb_2F_{11}^-$ with the displacement ellipsoids at the 50% probability level. The Br···F bridges result in a preferential compression of the equatorial F−Br−F angle and the formation of infinite zigzag chains along the *c*-axis.

Table 3. Atomic Coordinates ($\times 10^4$) and Equivalent Isotropic Displacement Parameters ($Å^2 \times 10^3$) for $BrF_4^+Sb_2F_{11}^-$[a]

	x	y	z	U(eq)
Sb(1)	5297(1)	6472(1)	3518(1)	23(1)
Sb(2)	2557(1)	8534(1)	5130(1)	22(1)
Br(1)	9167(1)	8510(1)	1861(1)	26(1)
F(1)	6574(7)	5587(2)	2720(2)	57(1)
F(2)	6881(5)	7453(2)	2865(2)	36(1)
F(3)	8081(6)	6430(2)	4312(2)	43(1)
F(4)	3511(6)	5655(2)	4262(2)	50(1)
F(5)	2400(5)	6688(2)	2798(2)	43(1)
F(6)	3984(5)	7462(2)	4366(2)	43(1)
F(7)	1149(6)	9424(2)	5882(2)	48(1)
F(8)	5461(6)	8373(2)	5849(2)	43(1)
F(9)	4238(6)	9286(2)	4287(2)	43(1)
F(10)	-224(6)	8436(2)	4329(2)	38(1)
F(11)	1073(5)	7564(2)	5847(2)	37(1)
F(12)	12022(7)	8638(2)	2465(2)	52(1)
F(13)	6324(6)	8613(2)	1243(2)	52(1)
F(14)	7971(6)	9297(2)	2590(2)	43(1)
F(15)	10410(5)	9237(2)	1077(2)	40(1)

[a] U(eq) is defined as one-third of the trace of the orthogonalized U^{ij} tensor.

Table 4. Bond Lengths and Angles for $BrF_4^+Sb_2F_{11}^-$

Bond Lengths (Å)

Sb(1)−F(3)	1.837(3)	Sb(2)−F(9)	1.845(3)
Sb(1)−F(1)	1.840(3)	Sb(2)−F(10)	1.847(3)
Sb(1)−F(4)	1.844(3)	Sb(2)−F(11)	1.905(3)
Sb(1)−F(5)	1.850(3)	Sb(2)−F(6)	2.039(2)
Sb(1)−F(2)	1.892(3)	Br(1)−F(14)	1.664(3)
Sb(1)−F(6)	1.998(2)	Br(1)−F(15)	1.667(3)
Sb(2)−F(7)	1.832(3)	Br(1)−F(12)	1.728(3)
Sb(2)−F(8)	1.840(3)	Br(1)−F(13)	1.729(3)

Bond Angles (deg)

F(3)−Sb(1)−F(1)	93.75(15)	F(8)−Sb(2)−F(10)	167.58(15)
F(3)−Sb(1)−F(4)	91.68(14)	F(9)−Sb(2)−F(10)	91.31(13)
F(1)−Sb(1)−F(4)	95.18(16)	F(7)−Sb(2)−F(11)	92.49(14)
F(3)−Sb(1)−F(5)	171.32(14)	F(8)−Sb(2)−F(11)	86.98(13)
F(1)−Sb(1)−F(5)	94.39(15)	F(9)−Sb(2)−F(11)	168.57(13)
F(4)−Sb(1)−F(5)	90.57(13)	F(10)−Sb(2)−F(11)	87.17(12)
F(3)−Sb(1)−F(2)	88.75(12)	F(7)−Sb(2)−F(6)	175.13(13)
F(1)−Sb(1)−F(2)	93.53(15)	F(8)−Sb(2)−F(6)	83.96(12)
F(4)−Sb(1)−F(2)	171.23(14)	F(9)−Sb(2)−F(6)	85.94(13)
F(5)−Sb(1)−F(2)	87.76(12)	F(10)−Sb(2)−F(6)	84.43(12)
F(3)−Sb(1)−F(6)	85.89(12)	F(11)−Sb(2)−F(6)	82.64(11)
F(1)−Sb(1)−F(6)	178.17(15)	F(14)−Br(1)−F(15)	97.48(16)
F(4)−Sb(1)−F(6)	86.63(13)	F(14)−Br(1)−F(12)	86.80(16)
F(5)−Sb(1)−F(6)	85.88(12)	F(15)−Br(1)−F(12)	85.68(15)
F(2)−Sb(1)−F(6)	84.67(11)	F(14)−Br(1)−F(13)	86.09(15)
F(7)−Sb(2)−F(8)	95.69(15)	F(15)−Br(1)−F(13)	86.78(15)
F(7)−Sb(2)−F(9)	98.94(15)	F(12)−Br(1)−F(13)	168.88(16)
F(8)−Sb(2)−F(9)	92.27(13)	Sb(1)−F(6)−Sb(2)	175.11(15)
F(7)−Sb(2)−F(10)	95.50(14)		

Table 5. Atomic Coordinates ($\times 10^4$) and Equivalent Isotropic Displacement Parameters ($Å^2 \times 10^3$) for $IF_4^+SbF_6^-$

	x	y	z	U(eq)
I(1)	5000	2500	1505(1)	16(1)
Sb(2)	0	2500	857(1)	13(1)
F(1)	3786(2)	1313(2)	2048(1)	27(1)
F(2)	3490(2)	4031(2)	1743(1)	32(1)
F(3)	0	2500	-42(2)	29(1)
F(4)	0	2500	1752(2)	25(1)
F(5)	2238(2)	2069(2)	857(1)	28(1)
F(6)	439(2)	4725(2)	853(1)	28(1)

[a] U(eq) is defined as one-third of the trace of the orthogonalized U^{ij} tensor.

bond distances and angles are summarized in Table 4. The BrF_4^+ cation adopts the expected distorted trigonal bipyramidal geometry in accordance with the structure (see graphic)

Table 6. Bond Lengths and Angles for $IF_4^+SbF_6^-$

Bond Lengths (Å)

I(1)−F(1)#1	1.7981(17)	Sb(2)−F(3)	1.853(4)
I(1)−F(1)	1.7981(17)	Sb(2)−F(6)#2	1.8846(17)
I(1)−F(2)	1.8490(17)	Sb(2)−F(6)	1.8846(17)
I(1)−F(2)#1	1.8490(17)	Sb(2)−F(5)#2	1.8854(17)
Sb(2)−F(4)	1.845(3)	Sb(2)−F(5)	1.8854(17)

Bond Angles (deg)

F(1)#1−I(1)−F(1)	103.06(12)	F(6)#2−Sb(2)−F(6)	179.53(12)
F(1)#1−I(1)−F(2)	80.48(9)	F(4)−Sb(2)−F(5)#2	90.00(6)
F(1)−I(1)−F(2)	80.53(8)	F(3)−Sb(2)−F(5)#2	90.00(6)
F(1)#1−I(1)−F(2)#1	80.53(8)	F(6)#2−Sb(2)−F(5)#2	89.82(7)
F(1)−I(1)−F(2)#1	80.48(9)	F(6)−Sb(2)−F(5)#2	90.18(7)
F(2)−I(1)−F(2)#1	149.24(13)	F(4)−Sb(2)−F(5)	90.00(6)
F(4)−Sb(2)−F(3)	180.0	F(3)−Sb(2)−F(5)	90.00(6)
F(4)−Sb(2)−F(6)#2	90.24(6)	F(6)#2−Sb(2)−F(5)	90.18(7)
F(3)−Sb(2)−F(6)#2	89.76(6)	F(6)−Sb(2)−F(5)	89.82(7)
F(4)−Sb(2)−F(6)	90.24(6)	F(5)#2−Sb(2)−F(5)	179.99(12)
F(3)−Sb(2)−F(6)	89.76(6)		

[a] Symmetry transformations used to generate equivalent atoms: #1 $-x+1, -y+{}^1/_2, z+0$; #2 $-x+0, -y+{}^1/_2, z+0$.

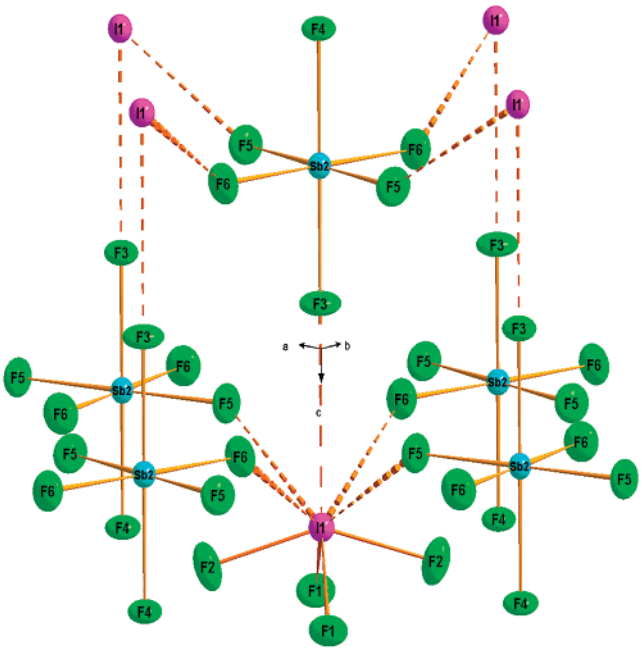

Figure 3. Crystal structure of $IF_4^+SbF_6^-$ with the displacement ellipsoids at the 50% probability level. The four shorter I···F bridges result in a preferential compression of the axial F−I−F angle and the formation of infinite polymeric sheets in the *xy*-plane.

predicted for AX_4E-type species by the VSEPR theory.[16] The F14, F15 atoms and the lone pair on Br1 form the equatorial plane. As in the case of ClF_4^+,[4] SF_4,[17] and SeF_4,[18] the axial bonds of ~1.73 Å are significantly longer than the equatorial bonds of ~1.66 Å, and their lengths are in excellent agreement with the theoretical predictions given in Table 2. Furthermore, the axial and equatorial F−Br−F angles of 168.9(2)° and 97.5(2)°, respectively, are significantly compressed from the ideal values of 180° and 120°. The

(16) Gillespie, R. J.; Hargittai, I. *The VSEPR Model of Molecular Geometry*; Allyn and Bacon: Boston, 1991. Gillespie, R. J.; Popelier, P. L. A. *Chemical Bonding and Molecular Geometry: from Lewis to Electron Densities*; Oxford University Press: Oxford, U.K., 2001.
(17) Tolles, W. M.; Gwinn, W. D. *J. Chem. Phys.* **1962**, *36*, 1119.
(18) Bowater, I. C.; Brown, R. D.; Burden, F. R. *J. Mol. Spectrosc.* **1968**, *28*, 454.

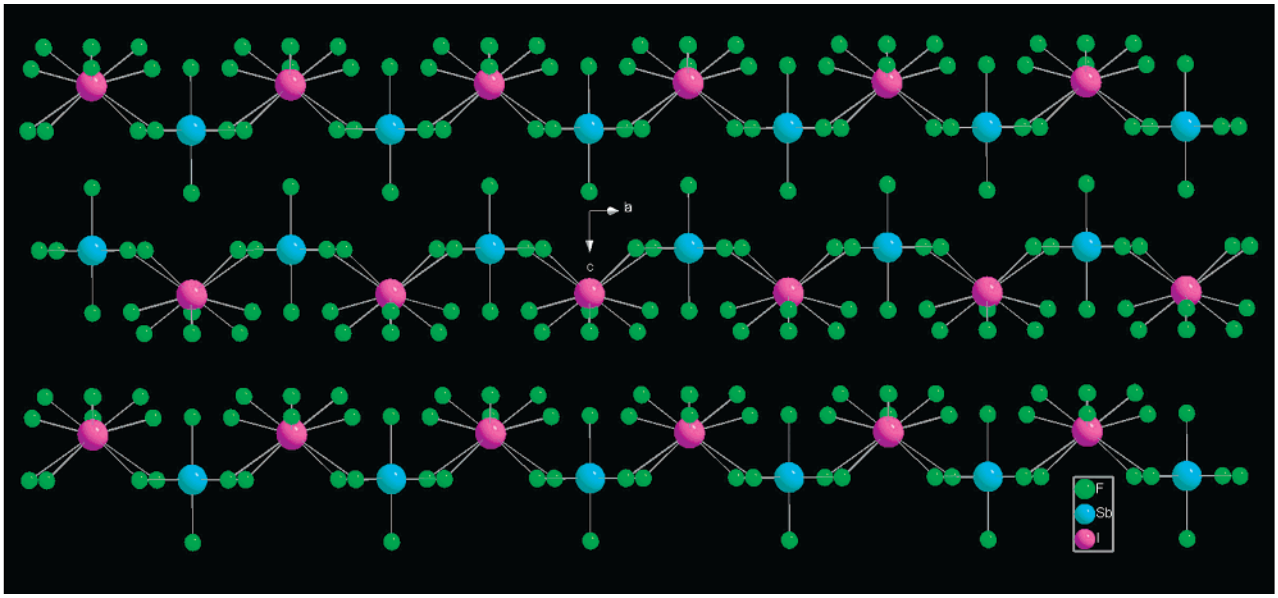

Figure 4. Packing diagram for $IF_4^+SbF_6^-$ showing the arrangement of the polymeric sheets that are perpendicular to the *yz*-paper-plane and their interconnection through the longer fluorine bridges. The iodine atoms are shown in purple, and the antimony atoms, in blue.

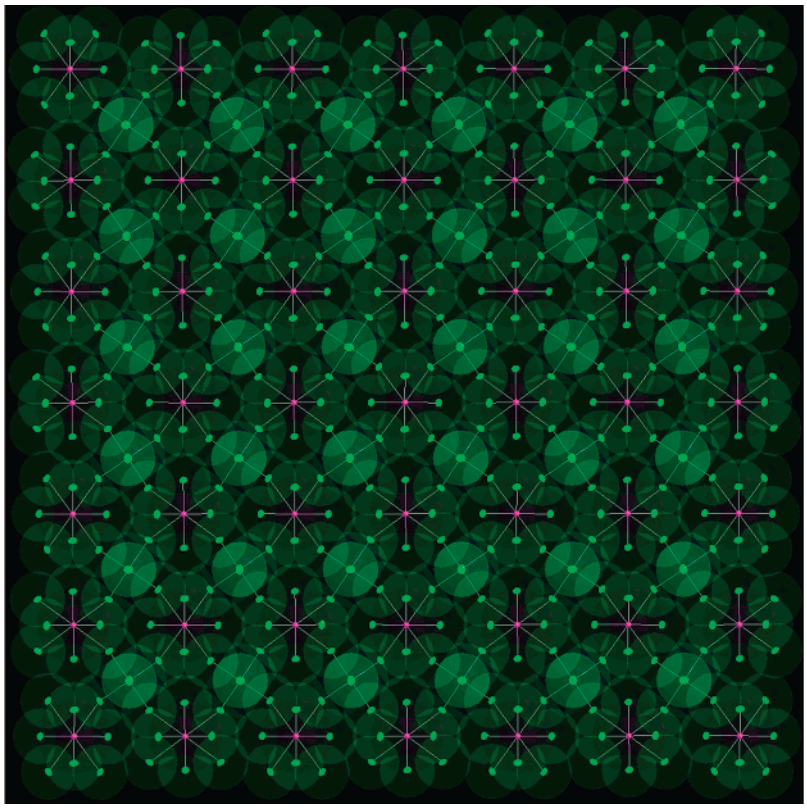

Figure 5. Crystal lattice of $IF_4^+SbF_6^-$ showing the highly symmetric arrangement along the *z*-axis with the iodine atoms in purple and the fluorine atoms in green. The "CD-changer" pattern is due to the van der Waals radii of the antimony atoms that are hidden by the axial fluorine atoms. The alternation of the direction of the "Viking hero's Skofnung battle axe" pattern is due to an alternation of the orientation of the IF_4 groups within the sheets.

coordination around bromine is completed by two close fluorine contacts of 2.414(3) Å (Br1···F2) and 2.347(3) (Br1···F11A) Å from two $Sb_2F_{11}^-$ anions, resulting in infinite zigzag chains of alternating cations and anions along the *c*-axis (see Figure 2). The bridge angle, Br···F−Sb, is ∼170°, and if the two fluorine bridges are included in the coordination sphere of bromine, its coordination number becomes 7. This fluorine-bridging mode closely resembles that previously found[4] for $ClF_4^+SbF_6^-$ and results in a preferential compression of the equatorial F−Br−F bond angle.

The geometry of the $Sb_2F_{11}^-$ anion depends strongly on the counterion and can vary from a linear, eclipsed, D_{4h}

(19) See for example: Willner, H.; Bodenbinder, M.; Broechler, R.; Hwang, G.; Rettig, S. J.; Trotter, J.; von Ahsen, B.; Westphal, U.; Jonas, V.; Thiel, W.; Aubke, F. *J. Am. Chem. Soc.* **2001**, *123*, 588 and references therein.

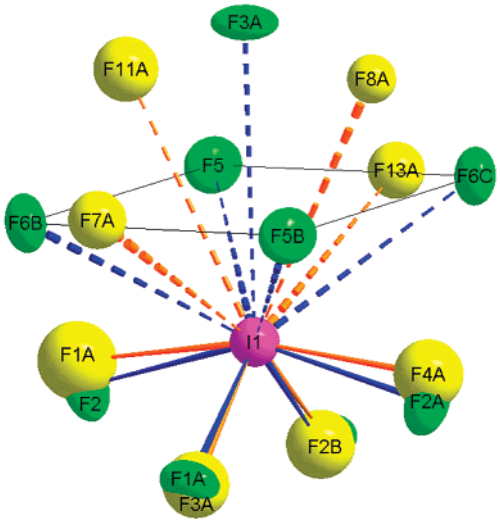

Figure 6. Comparison of the fluorine-bridging in $IF_4^+SbF_6^-$ (green) and $IF_4^+Sb_2F_{11}^-$ (yellow), showing the preferential compression of the axial F2−I1−F2A angle in the former and of the equatorial F3A−I1−F2B angle in the latter.

symmetry structure to strongly bent, staggered structures with an Sb−F−Sb angle of about 150° and dihedral angles of the equatorial SbF_4 groups of up to 50°.[19] In $BrF_4^+Sb_2F_{11}^-$, the $Sb_2F_{11}^-$ anion is present in a quasieclipsed conformation with an almost linear Sb1−F6−Sb2 bond of 175.1(1)°. The Sb1−F6−Sb2 bridge exhibits a slight asymmetry with Sb1−F6 and Sb2−F6 values of 1.998(2) and 2.039(2) Å, respectively. The fluorine atoms that are not involved in bridging have an average Sb−F bond distance of 1.842(3) Å, while the two bonds involving the two Sb−F···Br bridges are elongated to 1.899(3) Å.

Crystal Structure of $IF_4^+SbF_6^-$. Although Baird briefly reported a structure for this compound in 1969,[6] it was solved in the incorrect space group with a very low *R*-factor of 0.15, and no structural detail or complete refinement was ever published. The structure of $IF_4^+Sb_2F_{11}^-$ has also been reported,[7] but the accuracy was also low (*R*-factor of 0.09), and the bond angles found for IF_4^+ were very different from those reported by Baird. Furthermore, the $IF_4^+Sb_2F_{11}^-$ crystal had been obtained accidentally[7] in a reaction of CrO_2F_2 and SbF_5 with IF_5, and an improved bulk synthesis of this compound was desirable. Our attempt to prepare $IF_4^+Sb_2F_{11}^-$ by a 1:2 reaction of IF_5 and SbF_5 in HF solution resulted in the quantitative formation of $IF_4^+SbF_6^-$, and its crystal structure was determined. It crystallizes in the orthorhombic space group *Ibca*. The crystallographic data, atomic coordinates, equivalent isotropic displacement parameters, most important bond lengths and angles, and structure are given in Tables 1, 5, and 6 and Figure 3, respectively.

The structure of $IF_4^+SbF_6^-$ is predominantly ionic, containing fluorine-bridged IF_4^+ cations and SbF_6^- anions. However, the fluorine bridging in $IF_4^+SbF_6^-$ strongly differs from those in $ClF_4^+SbF_6^-$ and $BrF_4^+Sb_2F_{11}^-$. As can be seen from Figure 3, the IF_4^+ cation forms 4 shorter (2.70 Å) and 1 longer (3.01 Å) fluorine-bridge with 5 different SbF_6^- anions. This results in a monocapped, distorted square-antiprismatic, 9-coordinate environment around iodine. The imperfection of the square antiprism results from the 4 fluorine ligands of iodine not lying in a plane because of the difference in the $F_{ax}-I-F_{ax}$ and $F_{eq}-I-F_{eq}$ bond angles which also causes the twist angle of the two square faces to be 35.6° and not the ideal 45°. Because the axial fluorine

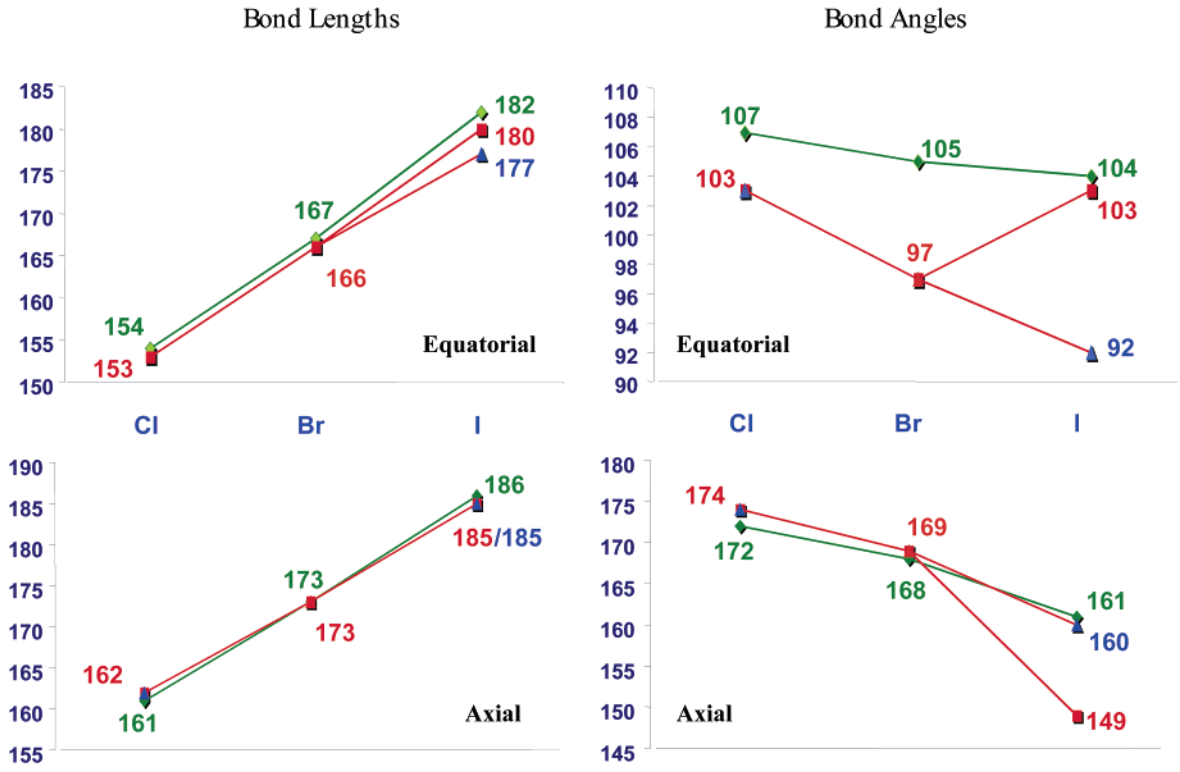

Figure 7. Comparison of the calculated and the redetermined experimental geometries for ClF_4^+, BrF_4^+, and IF_4^+, showing the good agreement between the calculated (green) and experimental (red) data. For IF_4^+, the red values are those reported for $IF_4^+Sb_2F_{11}^-$, while the blue ones are those for $IF_4^+SbF_6^-$. The only significant deviations are caused by a preferential compression of one bond angle in each compound due to interionic fluorine bridging.

ligands experience a much stronger repulsion from the fluorine bridges than the equatorial ones, the axial F−I−F angle is preferentially compressed, contrary to the preferential compression of the equatorial angles in the $ClF_4^+SbF_6^-$ and $BrF_4^+Sb_2F_{11}^-$ structures.

Packing diagrams of $IF_4^+SbF_6^-$ are shown in Figures 4 and 5. The packing consists of double layers of IF_4^+ cations and SbF_6^- anions, with each IF_4^+ cation bridging four SbF_6^- anions (see Figure 3) through the 4 shorter fluorine bridges within the *xy*-plane, resulting in the formation of a network of two-dimensional sheets. These polymeric sheets are interconnected along the *z*-axis by the long I1···F3A fluorine-bridges.

The $R(I-F_{ax})$ and $R(I-F_{eq})$ values of 1.849(2) and 1.798(2) Å, respectively, and the equatorial F−I−F bond angle of 103.06(12)° are in excellent agreement with the calculated gas phase values of 1.861 and 1.818 Å and 103.8°, respectively. The significant deviation of the observed axial F−I−F angle of 149.24(13)° from the calculated values of about 160° is due to the previously mentioned preferential compression of the axial angle by the fluorine bridges.

Whereas the I−F bond lengths in $IF_4^+SbF_6^-$, 1.849(2) and 1.798(2) Å, are in fair agreement with those of 1.85(4) and 1.77(3) Å, previously reported for $IF_4^+Sb_2F_{11}^-$,[7] the corresponding bond angles differ markedly. While in $IF_4^+SbF_6^-$ the equatorial F−I−F angle (103.06(12)°) is close to the calculated one (103.8°), in $IF_4^+Sb_2F_{11}^-$ the axial angle (160.3(1.2)°) is close to the theoretically predicted value of 160°, but the equatorial one (92.4(1.2)°) is much smaller than the predicted one of 103.8°. This discrepancy is due to the different nature of the fluorine bridging in $IF_4^+SbF_6^-$ and $IF_4^+Sb_2F_{11}^-$ (see Figure 6). In the former, the four shorter fluorine bridges are identical, whereas in the latter, there are two pairs of fluorine bridges, F11A/F8A and F7A/F13A, which form very different cone angles of 64° and 118°. The one with the wider cone angle, F7A−I1−F13A, closely approaches and almost eclipses the equatorial fluorine atoms, F3A and F2B, of IF_4^+, thereby preferentially compressing the equatorial F3A−I1−F2B angle.

Conclusion. The present study resolves all the problems raised by the previous study.[4] The revised bond lengths and angles of the ClF_4^+, BrF_4^+, IF_4^+ series (Table 2 and Figure 7) now show excellent agreement with the theoretical predictions, if the preferential compression of one specific bond angle (equatorial F−X−F in $ClF_4^+SbF_6^-$, $BrF_4^+Sb_2F_{11}^-$, and $IF_4^+Sb_2F_{11}^-$, and axial F−X−F in $IF_4^+SbF_6^-$) in each structure due to strong anion−cation interactions is taken into consideration. Because the nature of the fluorine bridging strongly depends on the counterion and crystal packing, a different angle may be compressed even for the same cation in different salts. This is demonstrated for $IF_4^+SbF_6^-$ and $IF_4^+Sb_2F_{11}^-$. Taking the relatively unaffected angles of each structure, that is, the axial F−I−F angle of 160° from $IF_4^+Sb_2F_{11}^-$ and the equatorial F−I−F angle of 103° from $IF_4^+SbF_6^-$, the theoretical predictions for free IF_4^+ are well duplicated. As expected, the angle compression due to fluorine bridging becomes more pronounced with increasing size and softness of the central atom; that is, it increases from chlorine to iodine. The results of this study demonstrate the value of theoretical calculations for the detection, correction, and rationalization of experimental inconsistencies.

Acknowledgment. The authors thank Dr. Robert Corley for his steady encouragement and the National Science Foundation, the Defense Advanced Projects Agency, and the Air Force Office of Scientific Research for financial support.

Supporting Information Available: Tables of structure determination summary, atomic coordinates, bond lengths and angles, and anisotropic displacement parameters of $BrF_4^+Sb_2F_{11}^-$ and $IF_4^+SbF_6^-$ in CIF format. This material is available free of charge via the Internet at http://pubs.acs.org.

IC025900Q